MASS FLUX IN THE ECLIPTIC PLANE AND NEAR THE SUN DEDUCED FROM DOPPLER SCINTILLATION

Richard Woo
Jet Propulsion Laboratory, California Institute of Technology, Pasadena, California

Paul R. Gazis
San Jose State University Foundation, NASA Ames Research Center, Moffett Field, California

Abstract, During the late declining phase of the solar cycle, the tilt of the solar magnetic dipole with respect to the Sun's rotation axis leads to large-scale organization of the solar wind, such that alternate regions of high- and low- speed solar wind are observed in the ecliptic plane, In this paper, we use Doppler scintillation measurements to investigate mass flux of these two types of solar wind inside 0.3 AU, where in situ measurements have not been possible. We find that mass flux in high-speed streams: (1) is lower (by a factor of approximately 2.2) than the mass flux of the average solar wind in the heliocentric distance range of 0.3-0,5 AU, (2) is lower still (by as much as a factor of about 4) than the mass flux of the slow solar wind associated with the streamer belt, and (3) appears to grow with heliocentric distance. These Doppler scintillation results are consistent with the equator to pole decrease in mass flux observed in earlier spectral broadening measurements, and with trends and differences between high- and low- speed solar wind observed by in situ measurements in the range of 0.3- 1.0 AU. The mass flux results suggest that the solar wind flow in high-speed streams is divergent near the Sun, becomes less divergent with increasing heliocentric distance, and is approximately radial beyond 0,3 AU. The variability of mass flux observed within equatorial and polar high-speed streams close to the Sun is strikingly low. This low variability implies that, as Ulysses currently ascends to higher latitudes and spends more time in the south polar high-speed stream after crossing the heliospheric current sheet, it can expect to observe a marked decrease in variations of both mass flux and solar wind speed, a trend that appears to have started already,

INTRODUCTION

Of the extensive in situ solar wind measurements that have been conducted in the ecliptic plane, those coinciding with the late declining phase of the solar cycle have probably contributed most to our knowledge and understanding of global large-scale structure of the solar wind. The reason is that during the approach to solar minimum, the Sun's polar regions are dominated by large coronal holes, which typically extend towards the equatorial regions in each hemisphere, and serve. as the sources of two long-lived recurrent high-speed streams, These streams are observed on opposite sides of the Sun in the ecliptic plane during each solar rotation [see e.g., Hundhausen, 1977]. This unique large-scale organization of solar wind structure is a consequence of the tilt of the solar dipole with respect to the Sun's rotation axis [Zhao and Hundhausen, 198 1; Mihalov et al., 1990; Suess et al., 1993; Gazis, 1993], and offers the opportunity to observe alternately high-speed streams and slow solar wind with in situ plasma measurements confined to the ecliptic plane. Comparison of these two types of wind is especially interesting because they are associated with contrasting regions on the Sun - the high-speed streams with coronal holes where the magnetic fields are open [Hundhausen, 1977], and the intervening slow solar wind with the streamer belt where the magnet ic fields are closed [Feldman et al., 1977, 198 1; Schwenn, 1990]. Unfortunately, investigations of the properties of these two types of wind closer to the Sun than 0.3 AU have not been possible because of the absence of in situ spacecraft measurements,

Recent studies based on remote sensing Doppler scintillation measurements by Pioneer Venus orbiter (PVO) in 1984, and in situ field and particle measurements at the orbits of Venus and Earth, reveal that the alternating large-scale high-speed streams and slow solar wind, which are observed in the ecliptic plane during the late declining phase of the solar cycle, appear inside 0.3 AU as sharply divided scintillation regions, distinguished by the absence and presence of scintillation enhancements, respectively [Woo and Gazis, 1993]. Furthermore, the scintillation enhancements in the slow solar wind appear to be associated with coronal mass ejections (CMEs) observed in white-light coronagraphs. Evolution of solar wind structure with heliocentric distance is manifested by the apparent erosion and disappearance of scintillation enhancements in the slow wind within 0.4 AU, and the eventual formation of narrow regions of enhanced scintillation as a result of stream interaction at the leading edges of high-speed streams by 0.5 AU. It is clear that further information on the dynamic solar wind near the Sun based on these unique PVO measurements would be highly desirable. The purpose of this paper is to investigate mass flux and solar wind flow inside 0.5 AU by taking advantage of the fact that Doppler scintillation levels reflect mass flux [Woo and Schwenn, 1991].

DOPPLER SCINTILLATION

When a coherent spacecraft radio signal propagates through the turbulent solar wind, scattering by the electron density irregularities gives rise to fluctuations or scintillation in its observed phase and equivalently Doppler frequency. Wave propagation studies [Woo, 1978] have shown that when the electron density irregularities in the solar wind are described by a three-dimensional power-law spatial wavenumber spectrum with spectral index p, the rms Doppler scintillation σ_D is given by

$$\sigma_D \sim \Delta n_e \, v^{(p-2)/2} \tag{1}$$

where Δn_e is rms electron density fluctuation, and v is the solar wind speed transverse to the radio path (hence radial solar wind speed). Since σ_D responds to electron density fluctuation as well as solar wind speed, Doppler scintillation measurements contain information on both parameters of the solar wind, Spatial scales of the electron density irregularities, corresponding to the time scale range of 10 s to 3 min observed by Doppler scintillation measurements [Woo and Gazis, 1993], exhibit a wavenumber spectrum that is indeed power-law and close to Kolmogorov ($p = 11/3$) [Woo and Armstrong, 1979], so that

$$\sigma_D \sim A\, n_e\, v^{5/6} \qquad (2)$$

Since the radial dependence of Δn_e [Bourgois, 1969; Armstrong and Coles, 1978] and the mean electron density n_e [Bird and Edenhofer, 1990] both vary approximately as $1/R^2$ for heliocentric distances R greater than about 20 $R_\odot$, Δn_e is roughly proportional to n_e. If one makes the further approximation that $v^{5/6} \sim v$ (reasonable for wind speeds in the range of 300-1000 km/s), it can be seen that σ_D is approximately proportional to mass flux $n_e v$. Thus, Doppler scintillation serves as a proxy for mass flux. This has been demonstrated in comparisons of Doppler scintillation and in situ mass flux measurements of radially aligned solar wind plasma [Woo and Schwenn, 1991].

PIONEER VENUS DOPPLER SCINTILLATION MEASUREMENTS

We examine mass flux of the solar wind inside 0.5 AU using the 1984 Pioneer Venus Doppler scintillation measurements, all of which were essentially in the ecliptic plane. These measurements spanned nearly 4 months prior to the June 15, 1984 superior conjunction of Pioneer Venus, and probed heliocentric distances in the range of 18-115 $R_\odot$ (0.08-0.53 AU) off the west limb of the Sun. We use a time series of the 3 min σ_D measurements that has first been normalized to 1 AU by multiplying by $R^{1.5}$ (corresponding to $1/R^2$ dependence of Δn_e), then extrapolated to the Sun's surface assuming a constant radial solar wind speed of 450 km/s, and finally displayed according to Barrington longitude [see Figure 3 of Woo and Gazis, 1993].

We will investigate mass flux of the high-speed streams and slow wind separately inside 0.43 AU during Barrington rotations (CR) 1746-1748. Near the Sun, the high-speed streams and slow wind are manifested in Doppler scintillation as physically separate and sharply divided regions characterized by the absence (quiet scintillation) and presence (disturbed scintillation) of enhanced scintillation, respectively. 'I'his large-scale organization is consistent with the velocity measurements from the Helios spacecraft that show increasingly sharper divisions of high- and low-speed wind closer to the Sun (as close as 0.3 AU) [Schwenn, 1990]. Inside 0.3 AU (CR 1747-1748), the high-speed stream regions coincide approximately with Barrington longitudes 0-30° and 140-200°, while the slow wind regions coincide with Barrington longitudes 30-140° and 200-350°. Farther from the Sun and in the heliocentric distance range of 0.3-0.43 AU (CR 1746), high-speed streams and slow wind are not as readily identified based on enhanced scintillation. On the other hand, since the solar wind velocity profile does not change significantly over a narrow range of heliocentric distances, we will assume that the longitudes of the high-speed streams and slow wind during CR 1746 are the same as those during CR 1747-1748. The times, heliocentric distances, and solar longitudes of the high-speed streams and slow wind considered in this paper are summarized in Table 1,

For each of the high-speed stream and slow wind intervals listed in Table 1, we have computed the mean, standard deviation, and standard error of the mean of σ_D. Displayed in Figure 1 are the results for the mean and standard error of the mean (as error bars) in terms of heliocentric distance, where heliocentric distance is the average of the corresponding heliocentric distance range. The solid symbols pertain to the fast wind and the hollow ones to the slow wind, Like symbols are used to represent the same longitude range (e.g., solid circles for recurring high-speed stream at 140-200° solar longitude). Despite the uncertainties, it is clear from Figure 1 that the mean levels of σ_D (and hence mass flux) of the slow wind are higher (by as much as a factor of four) than those of the high-speed streams. The standard variation of σ_D, which characterizes the variability of mass flux, is 30% in the case of the high-speed streams and 100% for the slow wind.

We have computed the statistics of the time series of σ_D beyond 0.3 AU and covering the heliocentric distance range of 70-115 R. (CR 1745-1746). We regard this as the average solar wind because in situ mass flux [Schwenn, 1990] and phase scintillation [Armstrong et al., 1979] have both shown that beyond 0.3 AU the long-term solar wind in the ecliptic plane is approximately spherically symmetric and the flow is nearly radial. The shaded rectangle in Figure 1 represents the. results of σ_D for the average solar wind. The horizontal line through the center of the rectangle represents the mean, the width of the rectangle represents the heliocentric distance range over which the mean was computed, and the height of the rectangle represents the deviation from the mean (± the standard error of the mean). Inside 0.3 AU, the mass flux levels of the high-speed streams (emanating from equatorial coronal holes) shown in Figure 1 are about a factor of 2.2 lower than this average. This is consistent with similar equator-to-pole decreases in mass flux inferred during solar minimum conditions from spectra] broadening measurements inside 10 R_O [Woo and Goldstein, 1994] and from Lyman a measurements relevant to near 1 AU [Lallement et al., 1986]. Comparison of the mass flux results in Figure 1 inside 0.3 AU with those beyond 0.3 AU indicate that the flow of high-speed streams near the Sun is diverging (as would be expected from open magnetic field coronal hole regions), but beyond 0.3 AU the flow approaches radial. This evolution is also evident in the radial variation of mass flux measurements within 0,3 AU as described below.

While the results in Figure 1 do not represent simultaneous measurements of mass flux for radially aligned solar wind at varying distances from the Sun, comparisons even at widely separated times are still meaningful since the high-speed streams are recurrent. A linear least squares fit to the fast wind results in the range of 20-90 R_O is shown as a short-dashed line in Figure 1. There is a tendency for mass flux to grow with radial distance within the high-speed streams, and the trend seems more apparent when results of individual streams are compared (e.g., compare solid circles), This provides further evidence that the divergent high-speed streams near the Sun become less divergent with increasing heliocentric distance. The slow wind is highly variable due to temporal variations resulting from its close association with coronal mass ejections [Woo and Gazis, 1993]. While it is difficult to arrive at a definite conclusion on account of this variability, a linear least squares fit (long-dashed line in Figure 1) suggests that mass flux may tend to decrease with heliocentric distance in the slow wind,

Investigations of mass flux relevant to high-speed streams and slow solar wind have been carried out using in situ measurements from IMP 7/8 at 1 AU [Feldman et al., 1977] and from Helios in the heliocentric distance range of 0,3- 1.0 AU [Schwenn, 1990]. In these studies, fast and slow wind are categorized as either high or low speed based on solar wind speed. One of the results of this categorization is to effectively narrow the longitudinal ranges of the fast and slow wind by excluding intermediate-speed solar wind that has undergone dynamic interaction at the boundaries of the fast and slow wind, Remarkably, the mass flux results obtained from these observations beyond 0.3 AU are similar to those in Figure 1 inside 0.3 AU, though they show trends and relative differences between fast and slow wind that are smaller. Based on these measurements, mass flux in the fast wind is lower than that of both the average solar wind (by a factor of 1.4) and the slow wind (by a factor of 1.8). The variability in mass flux, as characterized by its standard deviation, is lower in the fast wind (15% for IMP 7/8, less than 55% for Helios) than in the slow wind (38% for IMP 7/8, 55% for Helios). The Helios results also show that mass flux grows with heliocentric distance by some 15% within the fast wind, and tends to decrease accordingly in the slow wind. Beyond 0.3 AU, these in situ measurements show that while vestiges of non-radial flows remain, evolution of the fast wind towards a radial flow continues.

DISCUSSION AND CONCLUSIONS

During the declining phase of the solar cycle, results from Doppler scintillation inside 0.3 AU show that mass flux in high-speed streams (1) is lower (by a factor of approximately 2.2) than the mass flux of the. average solar wind in the heliocentric distance range of 0.3-0.5 AU, (2) is lower still (by as much as a factor of 4) than the mass flux of the slow solar wind associated with the streamer belt, and (3) appears to grow with heliocentric distance. The reduced mass flux observed in equatorial high-speed streams is consistent with the equator-to-pole decrease in mass flux during solar minimum deduced from spectral broadening measurements of the solar wind near the Sun, and from Lyman alpha measurements of the solar wind near 1 AU. The Doppler scintillation results in the ecliptic plane are consistent with in situ mass flux measurements of high- and low-speed solar wind in the range of 0,3- 1.0 AU, but show larger relative differences and trends closer to the sun. These results suggest the solar wind flow in high-speed streams in the ecliptic plane is divergent near the Sun, becomes less divergent with increasing heliocentric distance, and is approximately radial beyond 0.3 AU, In contrast with the fast wind, the radial variation of mass flux in the case of the slow wind is highly uncertain on account of the high variability of mass flux. Still, the results suggest that the slow wind may be convergent near the Sun, becoming less convergent with heliocentric distance, and approaching radial flow beyond 0.3 AU. The evolution of non-radial flows to radial flow and the apparent erosion of fine plasma structure [Woo and Gazis, 1993] inside 0.3 AU, suggest rearrangement of plasma between the high-speed streams from coronal holes and the slow wind from the streamer belt. If the observed equality of momentum and total energy fluxes of the high- and low-speed wind is not caused by intrinsic solar phenomena, it may be a consequence of this rearrangement.

In addition to mass flux reduction, the other striking feature of high-speed streams close to the Sun, where stream evolution is minimal, is the conspicuously low variability (30%) of mass flux. Not surprisingly, this result is similar to the low mass flux variability observed in Doppler scintillation measurements of polar high-speed streams close to' the Sun [Woo and Armstrong, 1992]. Since low variability of electron density fluctuations is also observed in polar high-speed streams [Bourgois and Coles, 1992], solar wind speed variations must also be reduced there. The low variability of mass flux in polar high-speed streams is consistent with the absence of CMEs at high latitudes during solar minimum [Howard et al, 1985; Hundhausen, 1993]. The reduction of mass flux variability in high-speed streams in general is also consistent with the lack of evidence linking CME activity and coronal holes [Harrison, 1990]. The Doppler scintillation observations of low mass flux variability in equatorial and polar high-speed streams implies that, as the Ulysses spacecraft currently ascends to higher latitudes and spends more time in the south polar high-speed stream after crossing the heliospheric current sheet, it can be expected to observe a marked decrease in variations of both mass flux and solar wind speed, a trend that appears to have alread y started (private communication B.E. Goldstein).

A simplified global picture of solar wind structure and flow during solar minimum is emerging based on high time resolution Doppler scintillation measurements. Near the Sun, where evolution is minimal, divergent equatorial and polar high-speed streams exhibit depressed levels of mass flux level and variability, and are void of CMEs. Over the streamer belt (where closed magnetic fields prevail and the scalar wind is slow) and near the heliospheric current sheet, much solar wind structure and variability exists, some of which represents the interplanetary manifestation of CMEs. In the ecliptic plane, the original physically separate high-speed streams and slow solar wind observed during the approach to solar minimum evolve in such a manner as to produce apparent erosion of structure in solar wind plasma inside about 0.3 AU, and to produce approximately radial solar wind flow and stream interactions beyond about 0.3 AU. It is clear that further Doppler scintillation measurements near the Sun, both in and out of the ecliptic plane, can play an important role in improving our understanding of the relationship between the streamer belt, the heliospheric current sheet, and CMEs, and its evolution with heliocentric distance and solar cycle.

Acknowledgments, It is a pleasure to acknowledge the outstanding support received from the Pioneer Venus Project and the NASA Deep Space Network, We are grateful to C. Chang for programming and data processing, G. Goltz for retrieval of archived Pioneer

Venus Orbiter data, R, Fimmel, 1.. Colin, R. Jackson, D. Lozier and R. Ryan for support, and especially J.W. Armstrong for valuable discussions. This paper describes research carried out at the Jet Propulsion Laboratory, California Institute of Technology, under a contract with NASA, and at NASA Ames.

REFERENCES

Armstrong, J.W. and W.A. Coles, Interplanetary scintillations of PSR 0531 +21 at 74 MHz, *Astrophys. J., 220, 346-352, 1978.*

Armstrong, J. W., R. Woo, and F.B. Estabrook, Interplanetary phase scintillation and the search for very low frequency gravitational radiation, *Astrophys. J., 230, 570-574, 1979.*

Bird, M.K. and P. Edenhofer, Remote sensing observations of the solar corona, in *Physics of the Inner Heliosphere 1,* eds. R. Schwenn and E. Marsch, pp. 13-97, Springer-Verlag, Berlin, 1990.

Bourgois, G., Scintillation interplanétaire des radiosources à 2695 MHz, *Astron. Astrophys., 2, 209-217, 1969.*

Bourgois, G. and W.A. Coles, Solar cycle changes in the turbulence level of the polar stream near the Sun, in *Solar Wind Seven,* eds. E. Marsch and R. Schwenn, pp. 1 SS-158, Pergamon Press, Oxford, 1992.

Feldman, W. C., J.R. Asbridge, S.J. Bame and J.T. Gosling, Plasma and magnetic fields from the Sun, in *The Solar Output and Its Variations,* ed. O.R. White, Colorado Associated University Press, Boulder, 1977.

Feldman, W. C., J.R. Asbridge, S.J. Bame, E.E. Fenimore and J. I'. Gosling, The solar origins of solar wind interstream flows: near-equatorial coronal streamers, *J. Geophys. Res.*, 86, 5408-5416, 1981, Gazis, P. R., Pioneer Venus and IMP 8 observations of the latitude dependence of the solar wind, *J, Geophys. Res.*, 98, 9391-9400, 1993.

Harrison, R, A., The source regions of coronal mass ejections, Solar *Phys., 126*, 185-193, 1990.

Hundhausen, A. J., An interplanetary view of coronal holes, in *Coronal Holes and High Speed Wind Streams, eel,* J. Il. Zirker, pp. 225-329, Colorado Associated University Press, Boulder, 1977.

Hundhausen, A, J., Sizes and locations of coronal mass ejections: SMM observations from 1980 and 1984-1989, *J. Geophys. Res.*, 98, 13177-13200, 1993.

Howard, R. A., N.R. Sheeley, Jr., N. R., M.J. Koomen and D.J. Michels, Coronal mass ejections: 1979-1981, *J, Geophys. Res.*, 90, 8173-8191, 1985.

Lallement, R., T.E. Holzer and R.J. Munro, Solar wind expansion in a polar coronal hole: Inferences from coronal white light and interplanetary Lyman alpha observations, *J. Geophys. Res.*, 90, 1413-1423, 1985.

Mihalov, J. D., A. Barnes, A.J. Hundhausen and E.J. Smith, Solar wind and coronal structure near sunspot minimum: Pioneer and SMM observations from 1985-1987, J. Geophys. Res., 95, 8231-8242, 1990.

Schwenn, R., Large-scale structure of the interplanetary medium, in *Physics of the Inner Heliosphere f,* eds. R. Schwenn and E. Marsch, pp. 99-181, Springer-Verlag, Berlin, 1990.

Suess, S. T., D.J. McComas and J.T. Hoeksema, Prediction of the heliospheric current sheet tilt: 1992-1996, *Geophys. Res. Lett.*, 20, 161-164, 1993.

Woo, R., Radial dependence of solar wind properties deduced from Helios 1/2 and Pioneer 10/11 radio scattering observations, *Astrophys. J., 219,727-739,* 1978.

Woo, R. and J.W. Armstrong, Observations of large-scale structure in the inner heliosphere with Doppler scintillation measurements, in *Solar Wind Seven,* eds. E. Marsch and R. Schwenn, pp. 319-322, Pergamon Press, Oxford, 1992.

Woo, R. and P. Gazis, Large-scale solar-wind structure near the Sun detected by Doppler scintillation, *Nature*, 366, 543-545, 1993.

Woo, R. and R.M. Goldstein, Latitudinal variation of speed and mass flux in the acceleration region of the solar wind inferred from spectral broadening measurements, *Geophys. Res. Lett.*, in press.

Woo, R. and R, Schwenn, Comparison of Doppler scintillation and in situ spacecraft plasma measurements of interplanetary disturbances, *J. Geophys. Res.*, *96, 21227*-21244, 1991.

Zhao, X,-P. and A.J. Hundhausen, Organization of solar wind plasma properties in a tilted, heliomagnetic coordinate system, *J. Geophys. Res.*, 86, 5423-, 1981.

Table 1 Summary of high-speed stream and slow solar wind regions

Barrington Rotation Number	Time Interval, hrs UT	Heliocentric Distance range, solar radii	Barrington Longitude Range, degrees
Disturbed Scintillation Regions Slow Solar Wind			
1748	124.7 -136.5	32.0 -43,3	200-350
1748	140.9 -149,3	19.0 -27.4	30-140
1747	96.8 -108,5	58.6 -69.0	200-350
1747	113.1 -121.9	46.1 -54.4	30-140
1746	68.9 -80.6	83.0 -92.0	200-350
1746	85.2 -94.0	71.0 -79.0	30-140
Quiet Scintillation Regions High-Speed Streams			
1748	136.3- 141.0	27.4 -32.0	140-200
1748	149.3 - 151.1	17.2- 19.0	0-30
1747	108.5 -113,1	54.4 -58.6	140-200
1747	121,9- 123.8	44.3 -46.1	0-30
1746	80.6 -85.2	79.0 -83.0	140-200
1746	94.0 -95.7	70.0 -71.0	0-30

FIGURE CAPTIONS

Figure 1. The means and standard errors (error bars) of rms Doppler scintillation σ_D (which is proportional to solar wind mass flux) scaled to 1 AU as a function of heliocentric distance. Corresponding ranges of solar longitude and heliocentric distance are provided in Table 1. The hollow symbols refer to the slow solar wind regions, while the solid symbols refer to the high-speed streams. Like symbols (triangles or circles) indicate observations that cover the same solar longitude range. The shaded rectangle covers the approximate heliocentric distance range of 0.3-0.5 AU, and represents the results of the average solar wind. Long and short dashed lines represent the linear least squares fits to the results of the slow solar wind and high-speed streams, respective] y.

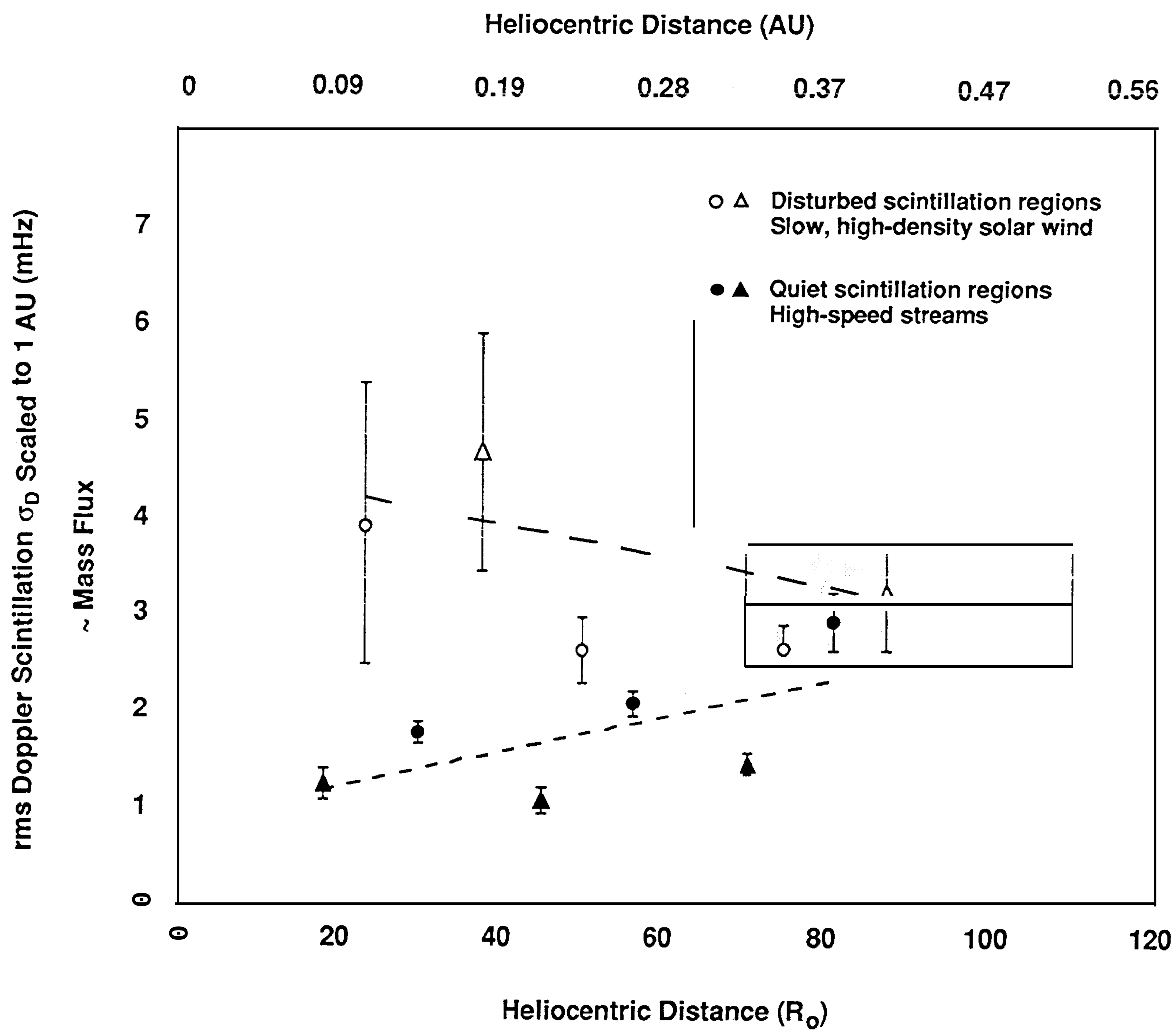

Heliocentric Distance (AU)
0
0.09
0.19
0.28
0.37
0.47
0.56
Disturbed scintillation regions
Slow, high-density solar wind
Quiet scintillation regions
High-speed streams
rms Doppler Scintillation σ_D Scaled to 1 AU (mHz)
~ Mass Flux
0
1
2
3
4
5
6
7
0
20
40
60
80
100
120
Heliocentric Distance (R_o)